JACS
JOURNAL OF THE AMERICAN CHEMICAL SOCIETY

COMMUNICATION

pubs.acs.org/JACS

Formation of a Strandlike Polycatenane of Icosahedral Cages for Reversible One-Dimensional Encapsulation of Guests

Johanna Heine,[†] Jörn Schmedt auf der Günne,[‡] and Stefanie Dehnen*[,†]

[†]Fachbereich Chemie and Wissenschaftliches Zentrum für Materialwissenschaften (WZMW), Philipps-Universität Marburg, Hans Meerwein Strasse, 35043 Marburg, Germany

[‡]Department of Chemistry, Ludwig-Maximilians-Universität München, Butenandtstrasse 5-13, D-81377 München, Germany

Supporting Information

ABSTRACT: Self-assembly of $ZnCl_2$ and the ligand 2,4,6-tris(4-pyridyl)pyridine (pytpy) in solution yields $[(ZnCl_2)_{12}(pytpy)_8]_n \cdot xCHCl_3$, a polycatenane consisting of a strand of mechanically interlocking icosahedral cages with an inner volume of more than 2700 Å^3. This can be used to encapsulate guest molecules of appropriate size and polarity, forming a precisely defined three-dimensional array of solvent nanodroplets within the crystalline framework. The dynamic composition of these droplets was studied using quantitative solid-state NMR spectroscopy.

The study of coordination cages, as part of the flourishing field of supramolecular chemistry, has attracted significant scientific attention. Known coordination cages feature many different polyhedral and prismatic geometries[1] ranging from small molecular boxes[2] to nanometer-sized Archimedean solids.[3] These supramolecular assemblies can be employed in molecular recognition and catalysis[4] and have been shown to act as templates for the synthesis of core−shell nanoparticles.[5] The related area of catenanes and rotaxanes, the perceived supramolecular building blocks of nanoscopic machines, has seen a similar amount of interest.[6] Nevertheless, despite substantial advances in both fields, only a few examples of catenated coordination cages are known. In 1999, Fujita's group showed that a [2]catenane can be generated from two different trigonal ligands and $[M(ethylenediamine)]^{2+}$ (M = Pd, Pt) units.[7] Nearly a decade later, Hardie et al. provided a second example, a triply interlocked [2]catenane based on a cyclotriveratrylene-type ligand and Zn^{2+} or Co^{2+} ions.[8] Lu and co-workers recently succeeded in synthesizing the first three-dimensional (3D) polycatenated framework constructed from adamantane-like coordination cages hosting Keggin polyoxometalate anions as templates.[9]

It had been our intention to gauge the reactivity of the currently very little used ligand 2,4,6-tris(4-pyridyl)pyridine (pytpy). The pytpy ligand is very closely related to the much more commonly employed tris(4-pyridyl)-1,3,5-triazine ligand (tpt), the only difference being the use of pyridine instead of triazine as the core (Chart 1).

Layering a chloroform solution of pytpy with a methanolic solution of $ZnCl_2$ yielded colorless hexagonal plates. Single-crystal X-ray diffraction (XRD) analysis showed the molecular formula to be $[(ZnCl_2)_{12}(pytpy)_8]_n \cdot xCHCl_3$ (**1**).[10] This compound represents a new kind of polycatenane consisting of a linear chain of interlocking icosahedral coordination cages based on the trigonal ligand and $ZnCl_2$ units. The structure of each cage has a $ZnCl_2$ unit at each of the 12 vertexes and eight pytpy ligands occupying the minimum number of trigonal planes necessary to connect all 12 $ZnCl_2$ units (Figure 1). The inner diameter of these cages is ∼20 Å.

Compound **1** represents the second reported example of an icosahedral coordination cage.[13,14] The asymmetric unit is composed of two $ZnCl_2$ units, a pytpy ligand and one-third of a second pytpy ligand [Figure S3 in the Supporting Information (SI)]. The result is that the ligands situated perpendicular to the crystallographic *c* axis are disordered because of the crystallographic symmetry. The position of the nitrogen atom in the core of the complete pytpy ligand may also be disordered, but this could not accurately be concluded from the diffraction data (see the SI for details).

The cages are connected not by any direct bonding interactions. Instead, they are interlaced, with a ligand-decorated plane of one coordination cage threaded through another, allowing for face-to-face $\pi-\pi$ interactions of the ligand cores (Figure 2). Each cage is connected in this way to two adjacent ones, forming a straight, infinite strand of cages along the crystallographic *c* axis. However, despite the additional space requirement of the interlacing neighbors, each cage still has a disk-shaped inner volume of more than 2700 Å^3 according to void calculations. While inorganic [*n*]catenanes of interlocking rings are rare but known,[17] **1** represents a step up in complexity as the first [*n*]catenane composed of cages.

These strands are closely packed within the rhombohedral unit cell; each strand is surrounded by six others, three shifted by $[0\ 0\ {}^1/_3]$ and three shifted by $[0\ 0\ -{}^1/_3]$ with respect to the first one (Figure 3 top). The centers of the cages form a distorted cubic close packing (ccp) motif (Figure 3 bottom).[18] The distortion is reflected by different center-to-center distances of 37.84 Å within one hexagonal layer and 22.47 Å between adjacent hexagonal layers. A significant compression along the crystallographic *c* axis leads to the closest center-to-center distance of 15.80 Å between two equivalent hexagonal layers, which is clearly different from the undistorted ccp structure. As a result of this packing, the empty planes of each icosahedral cage are either occupied by interlacing neighbors or $ZnCl_2$ units of adjacent strands.

XRD indicated a mobile content of the cages through the featureless form of the Fourier map. We therefore decided to perform a detailed solid-state NMR study, since NMR spectroscopy

Received: April 3, 2011
Published: June 09, 2011

Chart 1. Polypyridyl Ligands: (left) 2,4,6-Tris(4-pyridyl)-pyridine (pytpy); (right) Tris(4-pyridyl)-1,3,5-triazine (tpt)

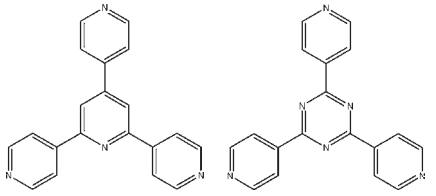

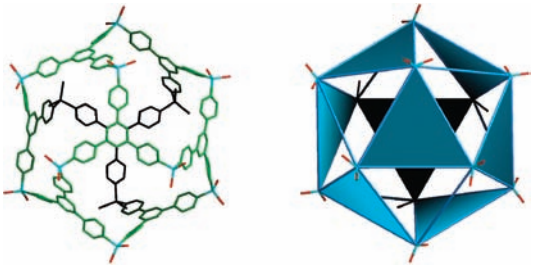

Figure 1. Icosahedral structure of the cage units in **1**. (left) Stick representation. Color code: Zn, blue; Cl, red; C and N, green. H atoms have been omitted for clarity. (right) Schematic drawing highlighting the icosahedral cage topology and the ligand decorated-triangular planes. Blue triangles represent the positions of the pytpy ligands.

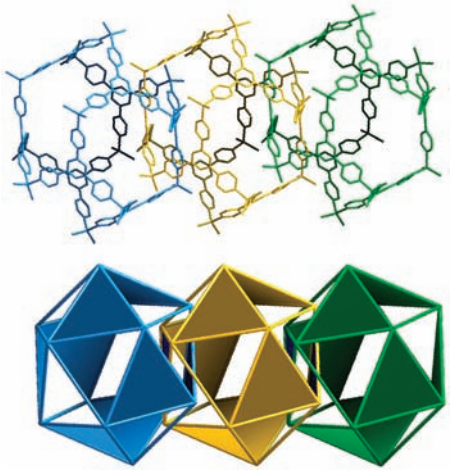

Figure 2. Structural fragment containing three interlaced icosahedral cages in **1**. (top) Stick representation of all atoms. (bottom) Schematic drawing highlighting the icosahedral cage topology and the ligand-decorated triangular planes. Two planes of each cage are involved in the catenation as a consequence of pytpy ligand $\pi-\pi$ interactions.

would be able to distinguish between the solvent and the framework molecules. The strategy was to use homonuclear and heteronuclear 2D correlation experiments to assign the peaks of the 1D ^{1}H NMR spectrum to H atoms of the solid framework and the molecules inside the voids. A washing procedure using another solvent allowed us to distinguish solvent molecules in the cages from solvent molecules that merely covered the particle surface. To simultaneously explore the inclusion capabilities of the cages, we conducted these experiments on a sample of **1** to which bromobenzene had been added as a potential guest during the

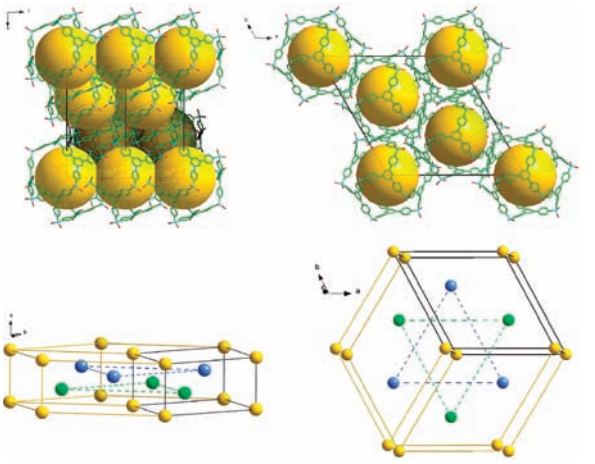

Figure 3. (top) Packing of the strands of interlaced coordination icosahedra in the crystal structure of **1**, viewed along the crystallographic *a* axis (left) and *c* axis (right). Yellow spheres represent the cavity volume of 2700 Å^3. It should be noted that the actual cavity shape is slightly oblate (see Figure S4 in the SI for a graphical representation). (bottom) Illustration of the distorted ccp topology of the icosahedral centers. Three unit cells are shown, with the A (yellow), B (green), and C (blue) positions distinguished by different colors.

crystallization process to provide the inclusion compound $[(ZnCl_2)_{12}(pytpy)_8]_n \cdot x CHCl_3 \cdot y C_6H_5Br$ (**1a**) (see the SI for details). A 1D magic-angle-spinning (MAS) ^{1}H NMR spectrum of **1a** at a spinning frequency where spinning sidebands became negligible showed a number of peaks that had to be assigned to EtOH (washing agent), $CHCl_3$, bromobenzene, and the pytpy ligands.

Framework hydrogen atoms hardly moved on the NMR time scale. Therefore, the homonuclear dipolar ^{1}H$-^1$H interactions were strong and could be used to highlight the ^{1}H atoms in the backbone stemming from the pytpy ligand. This was achieved with a double-quantum-filtered 2D correlation experiment (Figure 4). In good agreement with literature data for the pure ligand,[19] broad peaks with a chemical shift of >6.5 ppm were assigned to pytpy.

Peak assignments were achieved using a 2D ^{13}C{^{1}H} cross-polarization (CP) heteronuclear correlation (HETCOR) experiment (Figure 4), wherein we observed peaks from both the backbone and the included solvent molecules. At the chosen contact time of 10 ms, solvent molecules also showed cross-peaks because of the nonzero ^{1}H$-^{13}$C *J* coupling. The relatively sharp ^{1}H NMR peaks of $CHCl_3$ (δ_{iso} = 6.7 ppm) and bromobenzene (δ_{iso} = 5.7 ppm) were assigned with the help of the ^{13}C$-^1$H cross-peaks. Comparison of samples exposed to different washing agents (MeOH, EtOH) indicated that peaks with chemical shift values of <4 ppm were related to EtOH and MeOH, which were located at the particle surface. Worthy of note is the shielding difference relative to $CHCl_3$ (δ_{iso} = 7.6 ppm in $CDCl_3$) and C_6H_5Br (δ_{iso} = 7.22, 7.18, 7.44 ppm) in ordinary organic solutions, which is in line with the increased shielding caused by the metal−organic framework structure.

This demonstrates the specific inclusion capability of **1**. Accordingly, CHN analysis and IR spectroscopy indicated that upon crystallization without any additions, several equivalents of chloroform solvent were confined in the crystal structure (see the SI). Moreover, the absence of any strong OH bands was in perfect agreement with the NMR observation that neither methanol

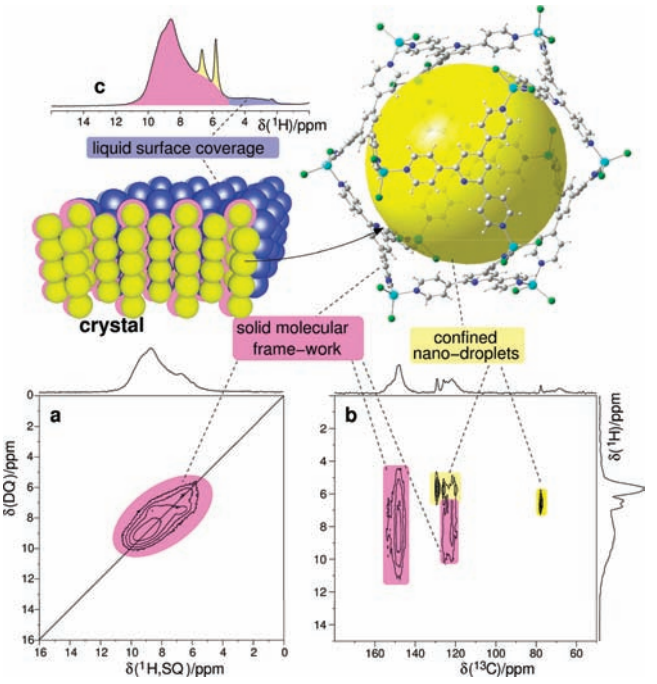

Figure 4. 2D solid-state MAS NMR spectra of **1a**. (a) ^{1}H 2D double-quantum (DQ)−single-quantum (SQ) correlation spectrum of **1a** at a spinning frequency of 50 kHz obtained using the BABA pulse sequence.[26] Because of the short excitation time of two rotor periods, only the nonmobile hydrogen atoms in the backbone of the pytpy ligand gave rise to sizable peaks in the DQ-filtered spectrum. The 1D spectrum shown at the top is a sum projection. (b) ^{13}C{^{1}H} 2D CP HETCOR MAS NMR spectrum of **1a** recorded with a contact time of 10 ms. Shown at the right is a 1D ^{1}H NMR spectrum with direct excitation, and the top spectrum is a sum projection over the full 2D spectrum. (c) Quantitative ^{1}H MAS NMR spectrum obtained with direct excitation.

nor ethanol was contained in the voids of the title compound. The high mobility of the encapsulated solvent molecules within the partially filled voids shows that there is only limited interaction between the cage and its contents. This also explains why we were unable to locate any reasonable positions for solvent molecules on the difference Fourier map during structure refinement. Thus, the structure corresponds to an ordered array of solvent-filled nanocapsules or an array of nanodroplets. This phenomenon is not without precedent: Robson and co-workers have reported that in a coordination polymer possessing a network structure with large, enclosed cavities, the confined solvent was in a quasi-liquid state.[20]

After assigning the peaks in the ^{1}H NMR spectrum, we used quantitative ^{1}H NMR spectroscopy[21] to study the uptake of solvent molecules. The ^{1}H NMR peak areas, observed on an as-made sample of **1a** washed with ethanol, were 110, 15.0, and 13.3 for pytpy, $CHCl_3$, and C_6H_5Br, respectively, meaning that the cages were filled with 15 $CHCl_3$ and 2.7 C_6H_5Br molecules on average. On the basis of the densities of pure $CHCl_3$ and $C_6H_5Br_3$, the volume occupied by the liquid phase was estimated to be 2490 Å^3; comparison to the volume of 2700 Å^3 estimated from the crystal structure indicates that the cages were almost completely filled. When this sample was dried in vacuum, however, the peak areas of the organic solvent and the framework molecules changed to 100, 1.1, and 7.1 for pytpy, $CHCl_3$, and C_6H_5Br, respectively, meaning that the cages contained only 1.2 $CHCl_3$ and 1.6 C_6H_5Br molecules on average.

On the basis of the peak assignments, we conclude that the small $CHCl_3$ molecules managed to escape from the $(ZnCl_2)_{12}(pytpy)_8$ cages but the only slightly bigger C_6H_5Br molecules were efficiently hindered by the framework structure, and as a result, a majority of them remained inside upon exposure of the sample to vacuum. The different volatilities of $CHCl_3$ and C_6H_5Br may also have contributed to this effect. Powder XRD patterns of the as-made and dried samples showed that the framework remained stable upon solvent removal (see the SI).

In contrast to the remarkable formation of **1**, the analogous reaction of tpt with zinc chloride under identical conditions yielded $[(ZnCl_2)_3(tpt)_2]_n$ (**2**) (see the SI), an extended network structure composed of twofold-interpenetrating 10^3-**ths** nets (with the tpt ligand as the 3-c nodes and the Zn as the spacer) of class IIa related by a center of inversion.[22] As the isostructural compounds $[(ZnX_2)_3(tpt)_2]$ (X = Br, I) were reported previously[23] and Robson and co-workers mentioned $[(ZnCl_2)_3(tpt)_2]$ earlier,[24] we would just like to add the crystallographic data for **2** to these findings. Additionally, reaction of $ZnCl_2$ and pytpy under solvothermal conditions yielded the 1D coordination polymer $[Zn(pytpy)Cl_2]_n$ wherein the $ZnCl_2$ units are connected via bridging pytpy ligands, leaving one pyridyl unit noncoordinating.[25] We observed the formation of a similar but not isostructural compound, $[Zn(pytpy)I_2]_n$ (**3**), when ZnI_2 instead of $ZnCl_2$ was employed in the reaction with pytpy (see the SI).

This poses the following question: Why did **1** form, if other seemingly more favorable structural motifs were available? From the employed reaction conditions, it is clear that the ligand core was the tipping point, and the use of pytpy shifted the formation process toward **1** as opposed to a structure analogous to $[(ZnCl_2)_3(tpt)_2]$. The pyridyl core enables direct face-to-face $\pi-\pi$ interactions, in contrast to the offset face-to-face interactions preferred by the more electron-deficient triazine core in interlocked Pd and Pt cages. The nature of the solvent within the cages was crucial to the formation of **1** as well. In the absence of a solvent of appropriate size and polarity, other structural motifs such as $[Zn(pytpy)Cl_2]$ become favored. Apparently the balance of interactions required to form **1** is so subtle that changing X in the ZnX_2 unit from Cl to I made **3** the favored motif. Naturally, we also attempted to employ $ZnBr_2$ as a building unit, but in that case we were unable to isolate any single-crystalline material.

An additional question also arises: Why was it possible to generate a polycatenane in our case, as opposed to the examples of [2]catenanes provided by Fujita and Hardie? We believe that the main factor was the charge neutrality of the $[(ZnCl_2)_{12}(pytpy)_8]$ cage. Both of the literature examples featured cages with a highly positive charge. This charge should effectively prevent further association of additional interlocking cages as a result of electrostatic repulsion and its neutralization by a protective hull of counterions. Another factor was the substantial inner volume of the icosahedral cages in **1**. While they require guests of a certain polarity and size, they are large and noninteracting enough to allow quasi-liquid behavior of their contents, reducing the "entropic penalty" paid for guest inclusion and demanding a less perfect fit than a similar cage of lesser volume. Additionally, the spacious arrangement of the cage framework easily allowed for the double catenation that led to the formation of **1**.

In summary, we have shown that through a minor variation of the employed ligand, vastly different structures may be obtained in the reaction of zinc halogenides with trigonal polypyridyl ligands, including an unprecedented strand of interlocking icosahedral cages. We have investigated the contents of these cages using

quantitative solid-state NMR spectroscopy, elucidating the selective nature of the guest uptake and quantifying the cage content under different conditions. Additionally, we have discussed the factors contributing to the formation of **1**, giving insight into design principles for other new, infinitely interlocked 3D assemblies. Future work will explore the inclusion of particular guest species such as radicals or fluorescent molecules as nanodroplets, enabling us to study confinement effects in these systems.

■ ASSOCIATED CONTENT

Supporting Information. Experimental details; details of crystal structure refinement and CIF files for **1**, **1a**, **2**, and **3**; details of the solid-state NMR investigation of **1a**; and additional characterization of **1**. This material is available free of charge via the Internet at http://pubs.acs.org.

■ AUTHOR INFORMATION

Corresponding Author
stefanie.dehnen@staff.uni-marburg.de

■ ACKNOWLEDGMENT

The authors thank the Deutsche Forschungsgemeinschaft (DFG) for financial support of this work. J.S.a.d.G. thanks Christian Minke (LMU) for technical assistance with the NMR spectrometer and the DFG for financial support through the Emmy-Noether Program (SCHM1570/2-1).

■ REFERENCES

(1) For example, see: (a) Caulder, D. L.; Raymond, K. N. *Acc. Chem. Res.* **1999**, *32*, 975. (b) Leininger, S.; Olenyuk, B.; Stang, P. J. *Chem. Rev.* **2000**, *100*, 853. (c) Dinolfo, P. H.; Hupp, J. T. *Chem. Mater.* **2001**, *13*, 3113. (d) Holliday, B. J.; Mirkin, C. A. *Angew. Chem., Int. Ed.* **2001**, *40*, 2022. (e) Cotton, F. A.; Lin, C.; Murillo, C. A. *Acc. Chem. Res.* **2001**, *34*, 759. (f) Swiegers, G. F.; Malefetse, T. J. *Coord. Chem. Rev.* **2002**, *225*, 91. (g) Seidel, S. R.; Stang, P. J. *Acc. Chem. Res.* **2002**, *35*, 972. (h) Gianneschi, N. C.; Masar, M. S., III; Mirkin, C. A. *Acc. Chem. Res.* **2005**, *38*, 825. (i) Fujita, M.; Tominaga, M.; Hori, A.; Therrien, B. *Acc. Chem. Res.* **2005**, *38*, 371.

(2) (a) Fujita, M.; Nagao, S.; Ogura, K. *J. Am. Chem. Soc.* **1995**, *117*, 1649. (b) Su, C.-Y.; Cai, Y.-P.; Chen, C.-L.; Smith, M. D.; Kaim, W.; zur Loye, H.-C. *J. Am. Chem. Soc.* **2003**, *125*, 8595–8613. (c) Yoshizawa, M.; Nakagawa, J.; Kumazawa, K.; Nagao, M.; Kawano, M.; Ozeki, T.; Fujita, M. *Angew. Chem., Int. Ed.* **2005**, *44*, 1810. (d) Ghosh, S.; Mukherjee, P. S. *Organometallics* **2008**, *27*, 316. (e) Zheng, Y.-R.; Zhao, Z.; Wang, M.; Ghosh, K.; Pollock, J. B.; Cook, T. R.; Stang, P. J. *J. Am. Chem. Soc.* **2010**, *132*, 16873. (f) Wang, M.; Zheng, Y.-R.; Ghosh, K.; Stang, P. J. *J. Am. Chem. Soc.* **2010**, *132*, 6282. (g) Wang, M.; Vajpayee, V.; Shanmugaraju, S.; Zheng, Y.-R.; Zhao, Z.; Kim, H.; Mukherjee, P. S.; Chi, K.-W.; Stang, P. J. *Inorg. Chem.* **2011**, *50*, 1506.

(3) Sun, Q.-F.; Iwasa, J.; Ogawa, D.; Ishido, Y.; Sato, S.; Ozeki, T.; Sei, Y.; Yamaguchi, K.; Fujita, M. *Science* **2010**, *328*, 1144.

(4) (a) Fiedler, D.; Leung, D. H.; Bergman, R. G.; Raymond, K. N. *Acc. Chem. Res.* **2005**, *38*, 351. (b) Yoshizawa, M.; Klosterman, J. K.; Fujita, M. *Angew. Chem., Int. Ed.* **2009**, *48*, 3418.

(5) Suzuki, K.; Takao, K.; Sato, S.; Fujita, M. *Angew. Chem., Int. Ed.* **2011**, *50*, 4858.

(6) *Molecular Catenanes, Rotaxanes and Knots*; Sauvage, J.-P., Dietrich-Buchecker, C., Eds.; Wiley-VCH: Weinheim, Germany, 1999.

(7) Fujita, M.; Fujita, N.; Ogura, K.; Yamaguchi, K. *Nature* **1999**, *400*, 52.

(8) Westcott, A.; Fisher, J.; Harding, L. P.; Rizkallah, P.; Hardie, M. J. *J. Am. Chem. Soc.* **2008**, *130*, 2950.

(9) Kuang, X.; Wu, X.; Yu, R.; Donahue, J. P.; Huang, J.; Lu, C.-Z. *Nat. Chem.* **2010**, *2*, 461.

(10) Single-crystal X-ray diffraction data: STOE IPDS2 diffractometer, graphite-monochromatized Mo Kα radiation (λ = 0.71073 Å), 100 K. Structure solution and refinement: direct methods and full-matrix least-squares on F^2, respectively; SHELXTL software.[11] Void calculations and treatment of the residual electron densities due to disordered solvent: PLATON software package.[12] Crystal data for **1**: $C_{160}H_{112}Cl_{24}N_{32}Zn_{12}$, M_r = 4118.06; trigonal, $R\bar{3}$; $a = b$ = 37.841(5) Å, c = 15.799(3) Å; V = 19592(5) Å^3; Z = 3; ρ_{calcd} = 1.047g cm^{-3}; μ(Mo Kα) = 1.365 mm^{-1}; 66080 reflns measured, 9195 unique; R(int) = 0.1621, R_1 [$I > 2\sigma(I)$] = 0.0811, wR_2 (all data) = 0.2312, S (all data) = 0.854. CCDC 809386. Additional details may be found in the SI.

(11) Sheldrick, G. M. *SHELXTL*, version 5.1; Bruker AXS Inc.: Madison, WI, 1997.

(12) Spek, A. L. *Acta Crystallogr.* **1990**, *A46*, c34.

(13) Brasey, T.; Scopelliti, R.; Severin, K. *Chem. Commun.* **2006**, 3308.

(14) In principle, the composition of eight planar tripodal ligands and 12 bidentate components may also yield a cuboctahedron. Several cuboctahedral coordination cages have been reported, both as singular units[15] and contained within a network of cages.[16] However, in the present case, the icosahedron is a more appropriate description because the windows of the cage, while quadrilateral in nature, deviate significantly from the planar square required for the formation of a cuboctahedron.

(15) (a) Olenyuk, B.; Whiteford, J. A.; Fechtenkötter, A.; Stang, P. J. *Nature* **1999**, *398*, 796. (b) Ghosh, K.; Hu, J.; White, H. S.; Stang, P. J. *J. Am. Chem. Soc.* **2009**, *131*, 6695.

(16) Inokuma, Y.; Arai, T.; Fujita, M. *Nat. Chem.* **2010**, *2*, 780.

(17) (a) Niu, Z.; Gibson, H. W. *Chem. Rev.* **2009**, *109*, 6024. (b) Fang, L.; Olson, M. A.; Benítez, D.; Tkatchouk, E.; Goddard, W. A., III; Stoddart, J. F. *Chem. Soc. Rev.* **2010**, *39*, 17. (c) Jin, C.-M.; Lu, H.; Wu, L.-Y.; Huang, J. *Chem. Commun.* **2006**, 5039. (d) Jin, C.-M.; Wu, L.-Y.; Lu, H.; Xu, Y. *Cryst. Growth Des.* **2008**, *8*, 215.

(18) Wells, A. F. *Structural Inorganic Chemistry*, 5th ed.; Oxford University Press: Oxford, U.K., 1984.

(19) Eichinger, K.; Nussbaumer, P.; Vytlacil, R. *Spectrochim. Acta, Part A* **1987**, *43*, 731.

(20) Batten, S. R.; Hoskins, B. F.; Robson, R. *J. Am. Chem. Soc.* **1995**, *117*, 5385.

(21) Avadhut, Y. S.; Schneider, D.; Schmedt auf der Günne, J. *J. Magn. Reson.* **2009**, *201*, 1.

(22) For the network nomenclature, see the following references: (a) O'Keeffe, M.; Peskov, M. A.; Ramsden, S. J.; Yaghi, O. M. *Acc. Chem. Res.* **2008**, *41*, 1782. (b) Blatov, V. A.; Carlucci, L.; Ciani, G.; Proserpio, D. M. *CrystEngComm.* **2004**, *6*, 377. (c) Baburin, I. A.; Blatov, V. A.; Carlucci, L.; Ciani, G.; Proserpio, D. M. *J. Solid State Chem.* **2005**, *178*, 2452.

(23) Biradha, K.; Fujita, M. *Angew. Chem., Int. Ed.* **2002**, *41*, 3392.

(24) Batten, S. R.; Robson, R. *Angew. Chem., Int. Ed.* **1998**, *37*, 1460.

(25) Wang, B.-C.; Wu, Q.-R.; Hu, H.-M.; Chen, X.-L.; Yang, Z.-H.; Shangguan, Y.-Q.; Yang, M.-L.; Xue, G.-L. *CrystEngComm.* **2010**, *12*, 485.

(26) Feike, M.; Demco, D. E.; Graf, R.; Gottwald, J.; Hafner, S.; Spiess, H. W. *J. Magn. Reson.* **1996**, *A122*, 214.